

## Reflectance spectroscopy of interplanetary dust particles

J. P. BRADLEY<sup>1\*</sup>, L. P. KELLER<sup>1</sup>, D. E. BROWNLEE<sup>2</sup> AND K. L. THOMAS<sup>3</sup>

<sup>1</sup>MVA Inc., 5500/200 Oakbrook Parkway, Norcross, Georgia 30093, USA

<sup>2</sup>Department of Astronomy, University of Washington, Seattle, Washington 98195, USA

<sup>3</sup>Lockheed, 2400 NASA Rd. 1, Houston, Texas 77058, USA

\*Correspondence author's e-mail address: jbrad@mindspring.com

(Received 1995 September 19; accepted in revised form 1996 February 14)

**Abstract**—Reflectance spectra were collected from chondritic interplanetary dust particles (IDPs), a polar micrometeorite, Allende (CV3) meteorite matrix, and mineral standards using a microscope spectrophotometer. Data were acquired over the 380–1100 nm wavelength range in darkfield mode using a halogen light source, particle aperturing diaphragms, and photomultiplier tube (PMT) detectors. Spectra collected from titanium oxide (Ti<sub>4</sub>O<sub>7</sub>), magnetite (Fe<sub>3</sub>O<sub>4</sub>), and Allende matrix establish that it is possible to measure indigenous reflectivities of micrometer-sized (>5  $\mu$ m in diameter) particles over the visible (VIS) wavelength range 450–800 nm. Below 450 nm, small particle effects cause a fall-off in signal into the ultraviolet (UV). Near-infrared (IR) spectra collected from olivine and pyroxene standards suggest that the  $\sim$ 1  $\mu$ m absorption features of Fe-bearing silicates in IDPs can be detected using microscope spectrophotometry.

Chondritic IDPs are dark objects (<15% reflectivity) over the VIS 450–800 nm range. Large (>1  $\mu$ m in diameter) embedded and adhering single mineral grains make IDPs significantly brighter, while surficial magnetite formed by frictional heating during atmospheric entry makes them darker. Most chondritic smooth (CS) IDPs, dominated by hydrated layer silicates, exhibit generally flat spectra with slight fall-off towards 800 nm, which is similar to type CI and CM meteorites and main-belt C-type asteroids. Most chondritic porous (CP) IDPs, dominated by anhydrous silicates (pyroxene and olivine), exhibit generally flat spectra with a slight rise towards 800 nm, which is similar to outer P and D asteroids. The most C-rich CP IDPs rise steeply towards 800 nm with a redness comparable to that of the outer asteroid object Pholus (Binzel, 1992). Chondritic porous IDPs are the first identified class of meteoritic materials exhibiting spectral reflectivities (between 450 and 800 nm) similar to those of P and D asteroids.

Although large mineral grains, secondary magnetite, and small particle effects complicate interpretation of IDP reflectance spectra, microscope spectrophotometry appears to offer a rapid, nondestructive technique for probing the mineralogy of IDPs, comparing them with meteorites, investigating their parent body origins, and identifying IDPs that may have been strongly heated during atmospheric entry.

### INTRODUCTION

Reflectance spectroscopy is an important discipline in solar system exploration. In the absence of samples, reflectance spectroscopy provides information about the surface compositions and mineralogy of planets, satellites, and comets. A large body of spectral data has been collected from the asteroids and, based on observed spectral reflectivities and geometric albedos, the asteroids have been classified into approximately 18 distinct classes (Tholen, 1984; Gaffey *et al.*, 1993). The most striking feature of asteroid classification is a pronounced gradation with increasing heliocentric distance (Gradie and Tedesco, 1982), which possibly results from a period of heating and metamorphism (with a strong radial gradient) during the early stages of solar system formation (Grimm and McSween, 1993; Brownlee, 1994). The S-class asteroids dominate the inner main belt, C-class the outer main belt, and P and D asteroids dominate the outer belt. It has been suggested that this gradation may persist throughout the solar system out to the dusty component of comets (*i.e.*, the spectral reflectivities of the ice-free components of comets are similar to those of some outer asteroids; Vilas and Smith, 1985; Jewitt and Luu, 1990).

Meteorites are derived mostly from asteroids, but their laboratory reflectance spectra suggest that they are a highly limited sampling. The bias is consistent with computed injection probabilities of asteroid fragments resulting from orbital resonances, which show that a large fraction of meteorites could be generated by a small ( $\sim$ 1%) fraction of the asteroid population (Farinella *et al.*,

1993). The reflectance of CI and CM meteorites ( $\sim$ 2% of meteorites) closely resembles that of main belt type-C asteroids (Johnson and Fanale, 1973; Vilas and Gaffey, 1989; Hiroi *et al.*, 1993a,b), but the unequilibrated ordinary chondrites (UOCs), which account for >75% of meteorite falls, have only one or two likely asteroid analogues (Gaffey *et al.*, 1993; Binzel *et al.*, 1993). Conversely, whole families of asteroids, including the outer P and D asteroids, have no spectral analogues among meteorites. Many of the outer asteroids exhibit characteristic low albedos and pronounced redness, which have been interpreted as evidence of the presence of organic materials rich in volatiles (Gradie and Ververka, 1980; Vilas and Smith, 1985; Binzel, 1992). Like comets, P and D asteroids may have escaped significant postaccretional alteration and, as such, may preserve evidence of early solar system and perhaps presolar processes. To date, no spectral analogues to outer P and D asteroids have been found among meteorites.

Interplanetary dust particles (IDPs) are micrometeorites 5–50  $\mu$ m in diameter that are collected in the stratosphere (Brownlee, 1986). Although IDPs appear to be derived from both asteroids and comets (Bradley and Brownlee, 1992; Keller *et al.*, 1992; Brownlee *et al.*, 1994, 1995), theoretical calculations, numerical simulations, and spacecraft observations have shown that the Earth is particularly effective at trapping unmelted asteroid dust (Flynn, 1989; Dermott *et al.*, 1994; Reach *et al.*, 1995). Asteroidal IDPs are expected to be a relatively unbiased sampling of the cumulative surface area of the dust-producing asteroids because, unlike large meteorites whose

orbits are determined solely by gravity, the orbits of asteroidal (and cometary) dust decay by Poynting-Robertson drag (Brownlee, 1994). Thus, identification of IDPs from a broad range of asteroidal parent bodies, comets, and other possible dust-producing objects are high priorities in interplanetary dust research. Larger 50–400  $\mu\text{m}$  micrometeorites collected from polar ices are also a potential source of unsampled parent bodies (Maurette *et al.*, 1993; Kurat *et al.*, 1993).

In principle, reflectance spectroscopy could be useful for determining the sources of IDPs. However, unlike meteorites, IDPs are extremely small objects with nanogram masses. A minimum sample size mass of 5 mg appears to have been the lower limit for reflectivity measurements on meteorites (Pieters *et al.*, 1993). At least some cometary IDPs have been distinguished from asteroidal IDPs by measuring their He release temperatures and, hence, their atmospheric speeds (Nier and Schlutter, 1990; Nier, 1994; Brownlee *et al.*, 1994, 1995). The mineralogy of three IDPs has been linked to CI and CM meteorites and, hence, a C-type asteroid origin (Bradley and Brownlee, 1992; Keller *et al.*, 1992; Rietmeijer, 1992). During the past three years, preliminary reflectance measurements of individual IDPs have been made (Bradley *et al.*, 1994; Bradley, 1994a; Brownlee *et al.*, 1994; Thomas *et al.*, 1995a). The data have been acquired using a microscope spectrophotometer, which requires limited sample preparation and performs the measurements nondestructively. In this paper, we present reflectance data on chondritic IDPs, a polar micrometeorite, and particulate mineral standards. The goals of this study are to: (a) demonstrate that indigenous reflectance properties of chondritic IDPs and individual fragments of IDPs can be measured; (b) extract useful mineralogical information from the reflectance spectra; and (c) make preliminary comparisons between the spectra of pristine IDPs and specific classes of asteroids.

## EXPERIMENTAL PROCEDURES

Interplanetary dust particles are simply mounted on glass microscope slides for the reflectance measurements. Spectra are acquired in darkfield mode using a microscope photometer (Zeiss MPM400) equipped with infinity corrected objectives and a DC stabilized 100 watt halogen light source. In darkfield mode, light is directed to the sample in a conical ring external to the imaging optics (*i.e.*, oblique incident illumination typically at an angle of 30 or 45° to the sample surface). Darkfield illumination, as opposed to brightfield illumination, minimizes reflectance from the substrate upon which the IDP is mounted (see Bradley, 1994a). Light scattered perpendicular to the slide surface is captured in the optical imaging path where it can be viewed and/or measured. The 50 $\times$  darkfield objective gives a field-of-view of 500  $\mu\text{m}$  in diameter in the binocular eyepieces. A photometry binocular tubehead allows the user to select a small portion of the field-of-view with a measuring diaphragm. The reduced field defines the area from which the signal will be detected, the size of which is adjusted according to the size of the IDP, thus eliminating any of the surrounding image information. This diaphragm can be seen in the field of view allowing precise positioning of the sample. Light that passes through the diaphragm opening is passed to the spectrophotometer unit where it first encounters a grating monochromator. The grating is motorized so that it may be controlled to place any portion of the full spectrum under the slit that enables automated scanning. Resolution is selectable from 1 to 20 nm, but for the IDP measurements, both 5 and 20 nm bandwidths were used. The light passing through the slit falls in on a photomultiplier detector which converts the light to an electrical signal. The signal is digitized and stored in the computer. A series of individual measurements are taken to build a complete spectrum.

Response characteristics of the microscope spectrophotometer and the two PMT detectors were determined by collecting spectra from a pressed barium sulfate ( $\text{BaSO}_4$ ) standard. ( $\text{BaSO}_4$  has a reflectance of 98% ( $\pm 0.5\%$ ) over the wavelength ranges measured.) Particulate mineral standards of titanium oxide ( $\text{Ti}_4\text{O}_7$ ), magnetite ( $\text{Fe}_3\text{O}_4$ ), serpentine, Fe-bearing olivine and pyroxene grains, and Allende (CV3) meteorite matrix were prepared. Titanium oxide was chosen because it is homogenous, it has a low bulk reflectivity, it is fine grained (average grain size is  $\sim 0.5 \mu\text{m}$  in diameter),

and its spectral response properties have also been measured elsewhere (C. Allen, pers. comm.). Pressed pellets of  $\text{Ti}_4\text{O}_7$ ,  $\text{Fe}_3\text{O}_4$ , olivine, pyroxene, and serpentine were prepared. Individual  $\text{Ti}_4\text{O}_7$  particles 10–50  $\mu\text{m}$  in diameter as well as 20–40  $\mu\text{m}$  diameter fragments of fine-grained, opaque matrix from the Allende meteorite were mounted on glass microscope slides.

Spectral measurements were performed over the visible and near IR 380–1100 nm wavelength range using two different photomultiplier tube (PMT) detectors (Fig. 1). The R928 detector is used in the spectral range 380–800 nm because of its high sensitivity. The less sensitive detector (R406) is used to extend the measurement range to  $\sim 1100$  nm. The R406 only became available towards the end of this study and it was used to explore the  $\sim 1 \mu\text{m}$  region where the "silicate features" of Fe-bearing olivines and pyroxenes occur (Burns, 1993; Pieters and McFadden, 1994).

## RESULTS

Figure 2 compares a bulk spectrum from a 2 mm region of a pressed pellet of  $\text{Ti}_4\text{O}_7$  with that of an individual 20  $\mu\text{m}$  diameter  $\text{Ti}_4\text{O}_7$  particle. (These spectra and all subsequent spectra of the visible 380–800 nm wavelength region were acquired using the R928 PMT detector.) Between  $\sim 450$  and 800 nm, the reflectivity of the particle mimics that of the bulk sample. Below 450 nm, the particle spectrum falls off into ultraviolet. This fall-off was observed with all  $\text{Ti}_4\text{O}_7$  particles measured, and a similar drop-off was observed with  $\text{BaSO}_4$ ,  $\text{Al}_2\text{O}_3$ , and  $\text{Fe}_3\text{O}_4$  (magnetite) particles. Figure 2 demonstrates that it is possible to determine the reflectivity of  $\text{Ti}_4\text{O}_7$  particles ( $< 25 \mu\text{m}$  in diameter) within 1% of the reflectivity of bulk  $\text{Ti}_4\text{O}_7$  between 420 and 800 nm.

Reflectance spectra from four fragments of Allende matrix are plotted in Fig. 3. The spectra were collected from particles between 20 and 40  $\mu\text{m}$  in diameter. The slopes and brightness (percent reflectivities) of the fragments are similar to bulk spectra of Allende and other CV3 meteorites (Hiroi *et al.*, 1993 a,b). Spectra of nine

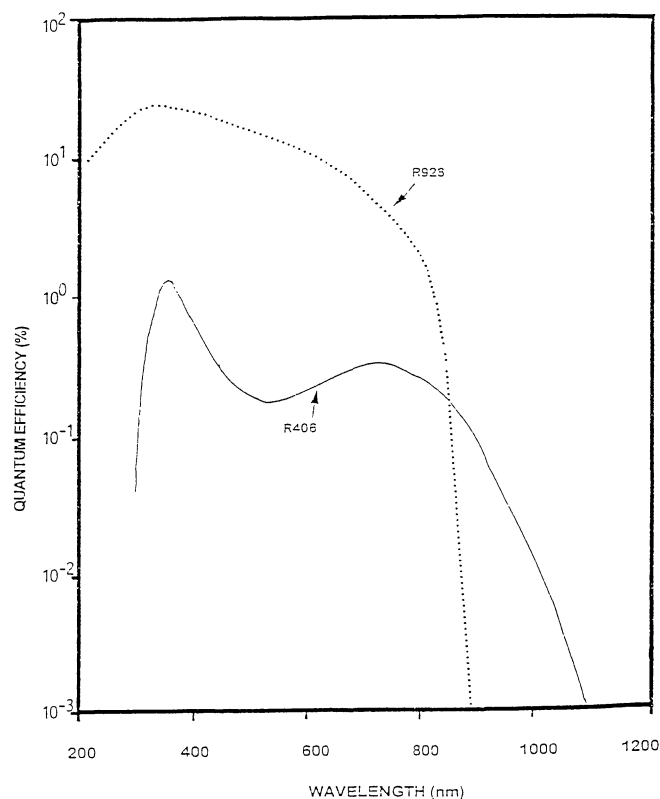


FIG. 1. Spectral response characteristics of the R928 and R406 photomultiplier (PMT) detectors. Data courtesy of Hamamatsu Corporation.

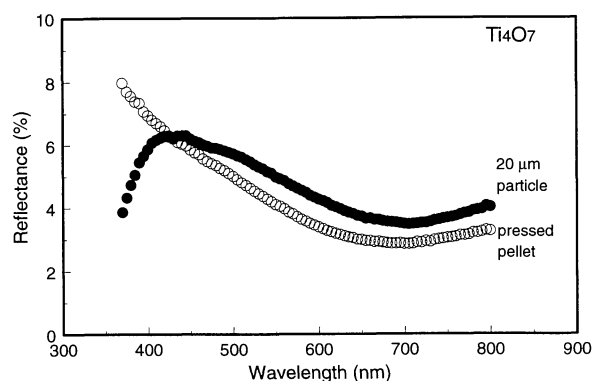


FIG. 2. Comparison of reflectance spectra from a pressed pellet of finely-ground  $\text{Ti}_4\text{O}_7$  and a  $20\ \mu\text{m}$   $\text{Ti}_4\text{O}_7$  particle. Note the fall-off below  $\sim 450\ \text{nm}$  in the particle spectrum. (Sample was provided by C. Allen, Lockheed, JSC.)

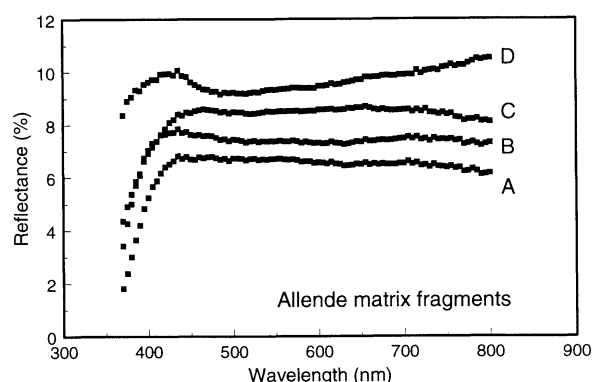


FIG. 3. Reflectance spectra from four  $20\text{--}40\ \mu\text{m}$  diameter fragments of matrix from Allende CV3 chondrite. Fragments B, C, and D are shifted upwards from A by 1, 2, and 3 reflectance units, respectively.

chondritic IDPs are shown in Fig. 4. The bulk compositions of the nine IDPs are listed in Table 1, and secondary electron (SEM) images of two of them are shown in Figure 5. Five of the IDPs belong to the chondritic smooth (CS) subset and four belong to the chondritic porous (CP) subset (Fig. 5). Chondritic smooth IDPs often contain hydrated (layer-lattice) silicates (smectite or serpentine), while CP IDPs usually contain only anhydrous silicates (pyroxene and olivine). (For reviews on mineralogical classification of chondritic IDPs see Brownlee *et al.*, 1982; Sandford and Walker, 1985; Bradley *et al.*, 1989; Schramm *et al.*, 1989; Germani *et al.*, 1990.) Note that five of the spectra, three in the CS group and two in the CP group, show a fall-off into the near IR (longwards of  $\sim 650\ \text{nm}$ ). Figure 6 is a transmission electron micrograph of an ultra-microtomed cross section of an IDP (L2006 A33) exhibiting such a fall-off. Note the presence of a "skin" of polycrystalline magnetite with a grain size on the order of  $50\text{--}100\ \text{nm}$  along the outer surface of the IDP. The magnetite was identified using electron diffraction and energy-dispersive x-ray spectroscopy (EDS). Since the abundance of magnetite in IDPs correlates with Zn depletions and He release temperature, it most likely forms as a result of frictional heating during atmospheric entry (Flynn *et al.*, 1992; Keller *et al.*, 1996).

Reflectance spectra from a  $\sim 60\ \mu\text{m}$  diameter chondritic micrometeorite recovered from an Antarctica ice core are plotted in Fig. 7. This micrometeorite, like other large polar micrometeorites, contains a semi-continuous  $1\text{--}3\ \mu\text{m}$  thick coating of magnetite over its surfaces (Kurat *et al.*, 1993; Maurette *et al.*, 1993). A spectrum was

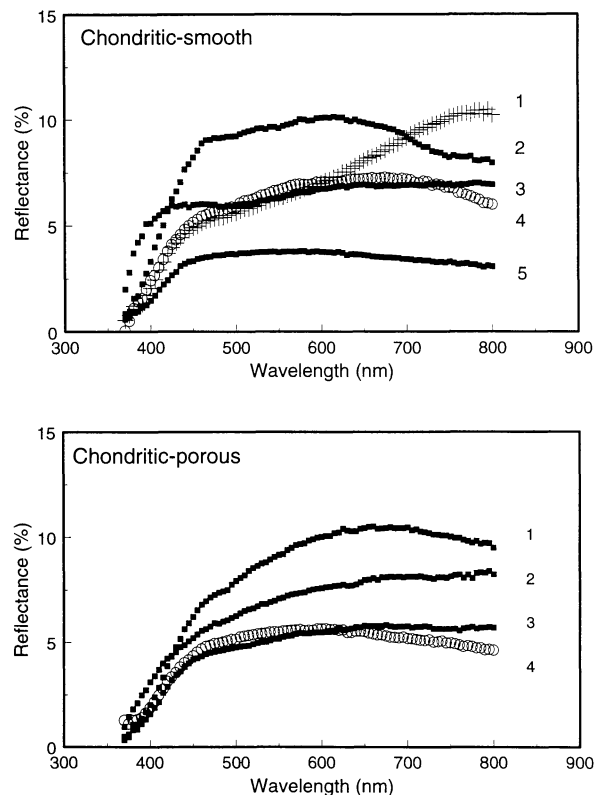


FIG. 4. Reflectance spectra from nine IDPs (compositions are listed in Table 1). (Upper) Chondritic smooth (CS) IDPs. (1) U2073A5B ( $\sim 5\ \mu\text{m}$  in diameter), (2) U2070A1B ( $9\ \mu\text{m}$  in diameter), (3) U2070A3D ( $15\ \mu\text{m}$  in diameter), (4) U2070A2H ( $9\ \mu\text{m}$  in diameter), (5) U2070A6A ( $8\ \mu\text{m}$  in diameter). (Lower) Chondritic porous (CP) IDPs. (1) U2073A5J ( $8\ \mu\text{m}$  in diameter), (2) U2073A7F ( $14\ \mu\text{m}$  in diameter), (3) U2070A2B ( $8\ \mu\text{m}$  in diameter), (4) U2070A8F ( $8\ \mu\text{m}$  in diameter). IDP diameter ( $\mu\text{m}$ ) is the average of the longest and shortest diameters.

first acquired from the surface. Then the micrometeorite was broken into several pieces, and a second spectrum was acquired from its core. The spectrum from the core rises sharply into the IR, but the rise is significantly diminished in the spectrum from the (magnetite-decorated) surface. For comparison, a spectrum of a  $20\ \mu\text{m}$  diameter magnetite particle is also shown in Fig. 7.

Reflectance spectra were also collected from fragments of several chondritic "cluster" IDPs. Cluster IDPs are large ( $\sim 20\text{--}100\ \mu\text{m}$  in diameter) IDPs that break into multiple fragments when they impact the collector surface. Figure 8 shows spectra from seven fragments of anhydrous cluster IDP L2005 #8. Although the spectral shapes from the seven fragments are similar, with slightly flat to reddened slopes, TEM studies showed that the fragments are compositionally and mineralogically diverse. Some exhibit chondritic element abundances, while others are dominated by single mineral grains (Thomas *et al.*, 1995a). The two brightest fragments (#39 and #111) have mineralogies dominated by single mineral grains (high-Ca clinopyroxene and FeNi-sulfide, respectively). (Brightness/darkness is defined as the total reflectance at  $560\ \text{nm}$ .) The C content of each fragment, determined using quantitative EDS (Thomas *et al.*, 1995a), is also tabulated in Fig. 8. The most C-rich fragments in L2005 are among the darkest, although the trend is not perfect. For example, the darkest fragment (312) contains 9 wt% C, but fragment 33, which contains 23 wt% C, is significantly brighter. Fragment 312 contains abundant magnetite, and another dark



TABLE 1. Major element compositions (normalized element wt%) of chondritic IDPs measured by energy dispersive x-ray analysis (see Figs. 4 and 5).

Sample #	Mg	Al	Si	P	S	K	Ca	Cr	Mn	Fe	Ni	O (by diff.)	Total
<b>Chondritic Smooth (CS)</b>													
U2070A-1B	13.85	9.99	12.65	0.53	4.81	0.00	1.30	0.00	0.00	17.01	1.30	38.57	100.1
U2070A-2H	9.32	0.60	9.17	0.00	14.23	0.00	0.34	0.53	0.00	24.22	13.49	28.10	100.0
U2070A-3D	9.83	1.19	14.72	0.00	6.93	0.00	0.00	0.00	0.00	31.96	1.50	33.86	99.99
U2070A-6A	12.40	1.44	17.06	0.39	4.79	0.00	0.00	0.00	0.51	24.06	2.46	36.89	100.0
U20703A-5B	15.95	1.03	15.66	0.00	0.00	na	1.27	0.00	0.00	26.88	1.36	37.84	99.99
<b>Chondritic Porous (CP)</b>													
U2070A-2B	12.41	1.25	15.69	0.00	11.89	0.33	1.11	0.00	1.37	20.34	1.35	34.26	100.0
U2070A-8F	12.58	0.59	15.26	0.00	11.68	0.00	1.00	0.39	0.83	22.62	1.23	33.83	100.01
U2073A-5J	20.51	3.54	17.13	0.00	1.72	na	0.65	0.00	0.00	14.63	0.94	40.87	99.99
U2073A-7F	10.94	0.88	13.44	0.00	13.26	na	0.77	0.00	0.00	26.98	1.88	31.84	99.99

fragment (37) that contains only 3 wt% C is also decorated with magnetite.

Figure 9 shows reflectance spectra of four fragments of chondritic cluster IDP L2006 #14. This cluster IDP is unusual in that all of the fragments in Fig. 9 have C-contents estimated to be at least 10× chondritic abundance. Volumetrically, amorphous C is the major constituent of fragment 10 followed by lesser low-Ca pyroxene and FeNi sulfides (Fig. 10). While the mass abundances of C in the fragments were not measured, related fragments from this cluster show 13× CI abundances of C (Thomas *et al.*, 1994). The carbo-

naceous material also contains GEMs (glass with embedded metal and sulfides; Bradley, 1994b). Electron energy-loss spectroscopy measurements show that the carbonaceous material is amorphous C with traces of N (Keller *et al.*, 1995). Polyaromatic hydrocarbons (PAHs) have also recently been identified in some chondritic IDPs (Allamandola *et al.*, 1987; Clemett *et al.*, 1993). The spectrum from the most C-rich fragment (10) and other fragments show a strong red slope characteristic of aromatic-rich carbonaceous materials and at least one outer asteroid (Fig. 9) (see Binzel, 1992; Luu *et al.*, 1994).

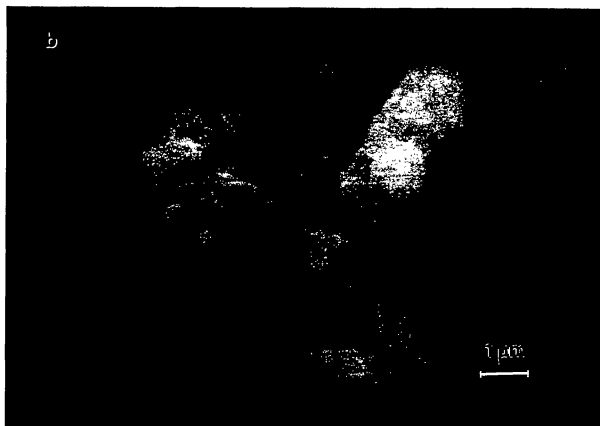
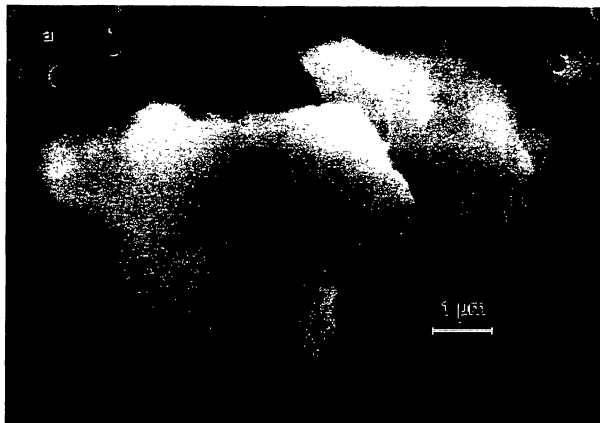


FIG. 5. Secondary electron images of (upper) hydrated (layer silicate-rich) CS IDP U2070A2H and (lower) anhydrous (pyroxene-rich) CP IDP U2073A7F.

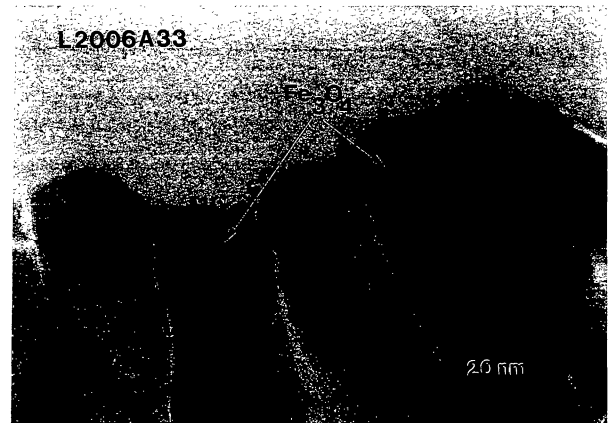


FIG. 6. Brightfield transmission electron micrograph of magnetite ( $\text{Fe}_3\text{O}_4$ ) on the surface of a partly melted chondritic IDP L2006 A33.

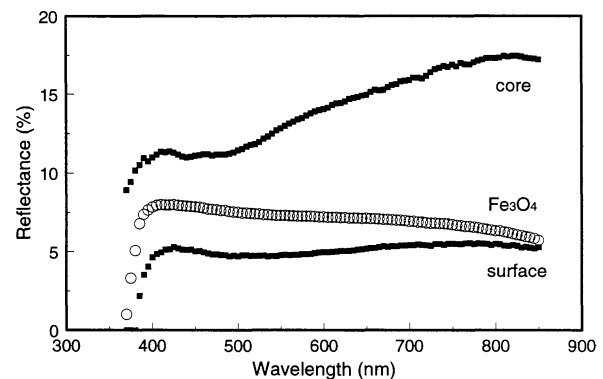


FIG. 7. Reflectance spectra from the surface of a  $\sim 65 \mu\text{m}$  diameter Antarctica micrometeorite (AMM), the core (an inner surface exposed after fracturing), and a magnetite ( $\text{Fe}_3\text{O}_4$ ) standard.

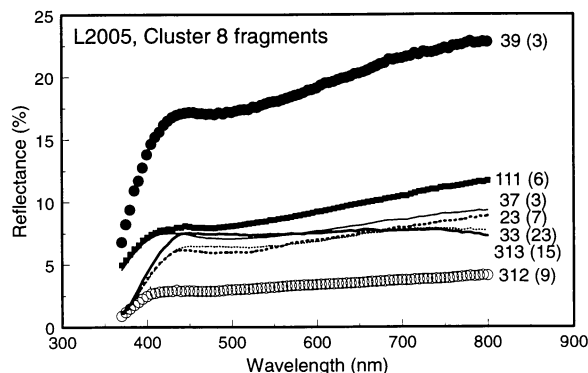


FIG. 8. Reflectance spectra from fragments of cluster IDP L2005 #8. Bulk C contents (element wt%) of each fragment are in parentheses.

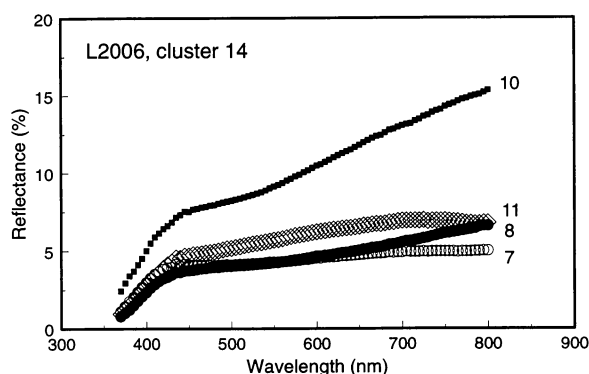


FIG. 9. Reflectance spectra from fragments of C-rich cluster IDP L2006 #14. Fragment 10 contains >90% C by volume (see Fig. 10).

Five fragments of cluster IDP L2005 #31 and four from cluster IDP L2011 #5 were also analyzed (Fig. 11). All fragments from L2005 #31 have similar bulk compositions including similar C-contents (Thomas *et al.*, 1995b). Differences in their reflectance spectra correlate with mineralogy. Fragments 1, 3, and 4 are anhydrous and dominated by pyroxene, while fragments 2 and 5 contain layer lattice silicates, which is indicative of aqueous alteration. Both of the layer lattice silicate-rich fragments show a pronounced fall-off in the near IR (Fig. 11, upper). Cluster IDP L2011 #5 is also a layer lattice silicate-rich (serpentine) particle. All fragments are compositionally similar to one another and the shapes of their reflectance spectra are largely similar (Fig. 11, lower). Between 450 and 800 nm, the overall spectrum of fragment 1 exhibits similarities to that of a serpentine standard (*cf.* Figs. 11, lower and 12).

Reflectance spectra were collected from three silicate mineral standards using the wider band R406 PMT detector. The purpose of these measurements was to determine whether the  $\sim 1 \mu\text{m}$  "silicate" features characteristic of octahedrally coordinated  $\text{Fe}^{2+}$  in olivines and pyroxenes can be detected using the microscope photometer. Figure 12 shows spectra from  $20 \mu\text{m}$  diameter regions of pressed pellets of finely-ground olivine, pyroxene, and serpentine. Although the olivine and pyroxene contain <10 mol%  $\text{Fe}^{2+}$ , absorption features at 900 nm and 1000 nm ( $1 \mu\text{m}$ ), respectively are clearly evident. The spectra of all three minerals correspond to those published elsewhere (Burns, 1993; Pieters and McFadden, 1994).

## DISCUSSION

The primary goal of this study has been to determine whether it

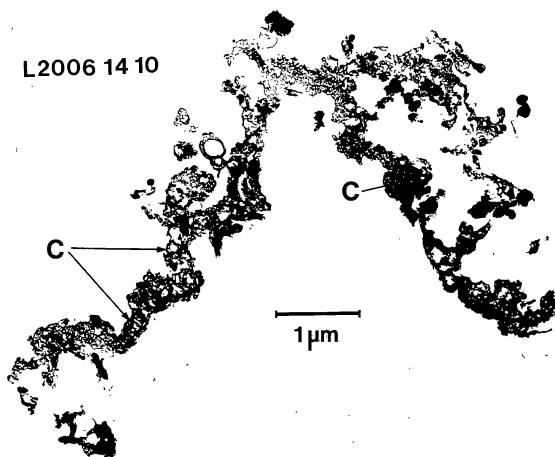


FIG. 10. Brightfield transmission electron micrograph of an ultramicrotomed thin-section of cluster IDP L2006 #14, fragment 10 supported on a  $\text{SiO}$  thin-film substrate. "C" is carbonaceous material which constitutes >90% of the volume of the IDP. This fragment was embedded and thin-sectioned in S rather than epoxy (see Bradley *et al.*, 1993). (The reflectance spectrum of fragment 10 is shown in Fig. 9.)

is possible to measure reflectance properties of micrometer-sized IDPs. Figures 2, 3, and 12 suggest that such measurements can be made, at least in the visible and near-infrared wavelength range 380–1100 nm, using darkfield illumination and a microscope spectrophotometer equipped with PMT detectors. In principle, the measurements can be expanded into the UV (<380 nm) and IR (>1100 nm) regions by incorporation of quartz optics and cooled PMT or solid-state detectors into the instrument. However, Fig. 2 indicates that small particles cause spectral artifacts in the UV. Between 450 and 800 nm, the reflectivity of the  $20 \mu\text{m}$   $\text{Ti}_4\text{O}_7$  particle matches that of the bulk material. Below 450 nm, there is an abrupt drop-off into the UV. The reason(s) for this drop-off are unclear, but a transition from a diffuse scattering condition to a specular condition is suspected. Alternatively, positioning aperturing diaphragms around the edges of small particles may cause spurious diffraction effects in the UV. Since this effect was observed with several particulate materials ( $\text{Ti}_4\text{O}_7$ ,  $\text{Al}_2\text{O}_3$ ,  $\text{BaSO}_4$ ,  $\text{Fe}_3\text{O}_4$ ) using both PMTs, UV spectral features below 450 nm should be treated with caution. Even with Allende matrix fragments, where a UV drop-off is characteristic of CV3 meteorites (*e.g.*, Hiroi *et al.*, 1993a,b), small particle effects cannot be excluded. Beyond 450 nm, however, each Allende fragment exhibits low brightness (<8% reflectivity) and generally flat spectra confirming that the reflectance of low-albedo, meteoritic particles can be accurately measured between 450 and 800 nm.

A second goal of this study was to evaluate whether the spectra of IDPs contain useful mineralogical information. If so, reflectance spectroscopy could provide a rapid, nondestructive method for classifying IDPs. Figures 4, 7, and 9 suggest that some spectra do contain mineralogical information. For example, several IDPs show a pronounced fall-off into the infrared beyond 650 nm. This effect is observed among CS IDPs, CP IDPs and even coarse-grained chondritic IDPs dominated by single mineral grains (*e.g.*, sulfides; Fig. 4). The drop-off was particularly common among a population of 57 IDPs containing a high number of larger (>15  $\mu\text{m}$  in diameter) particles (Bradley *et al.*, 1995). (Larger IDPs are typically heated to higher temperatures during atmospheric entry; Love and Brownlee, 1994.) Several IDPs exhibiting the effect were thin-sectioned and

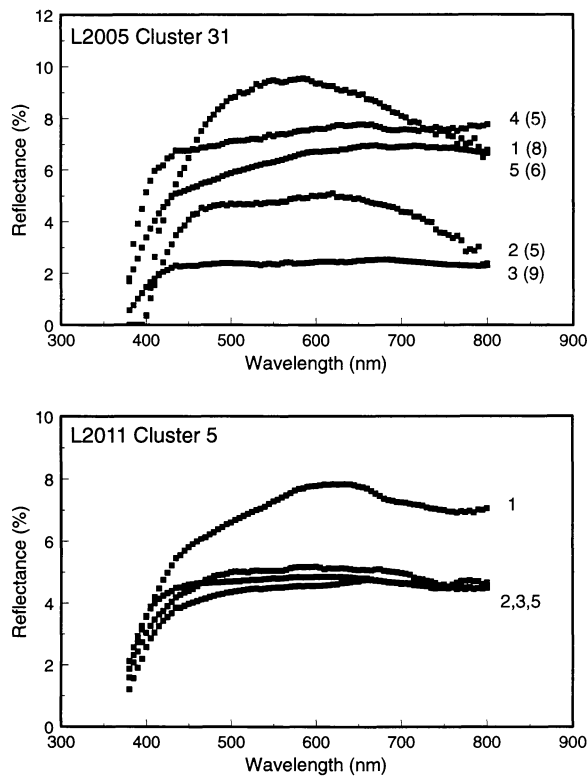


FIG. 11. Reflectance spectra from cluster IDPs (upper) L2005 #31 and (lower) L2011 #5. Fragments 1 and 2 contain hydrated silicates, while fragments 3, 4, and 5 contain only anhydrous silicates. Bulk C contents (element wt%) of each fragment are in parentheses.

found to contain magnetite coatings (e.g., Fig. 6), and the polar micrometeorite spectra clearly illustrate the effects of surficial magnetite (Fig. 7). Since there is evidence that magnetite is produced by strong heating during atmospheric entry (Flynn *et al.*, 1992), the near-IR drop-off may offer a rapid method for identifying heated IDPs. Unfortunately, magnetite may not be solely responsible for the effect. The spectra of some layer lattice silicates (e.g., serpentine) also exhibit a fall-off into the near-IR (Fig. 12). Magnetite was not detected in thin sections of IDP U20701B and cluster IDP L2005 #31 fragments 1 and 2, both of which show a pronounced drop-off (Figs. 4 and 11), although it is difficult to estimate the (three-dimensional) extent of magnetite formation on IDPs from examination of thin sections. Other specimen preparation and analysis techniques may be required to quantify the abundance of surface magnetite on IDPs and meaningfully assess its influence on reflectance spectra. If it turns out that magnetite is responsible for the near-IR fall-off, then reflectance spectroscopy can be used to identify strongly heated IDPs. On the other hand, attempts to measure indigenous spectral properties will need to be restricted to those IDPs that do not exhibit the drop-off. Fortunately, many IDPs appear to be in pristine condition; smaller 1–5  $\mu\text{m}$  in diameter IDPs are less likely to have been strongly heated, and there are clearly larger IDPs that do not exhibit the IR drop-off (Fig. 4). The influence of magnetite coatings on the reflectance properties of IDPs requires further investigation.

The silicate mineralogy of IDPs can also be probed using microscope photometry. Although the R406 is more than a factor of 10

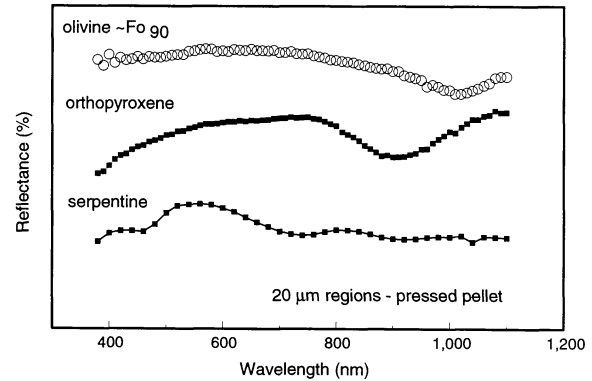


FIG. 12. Reflectance spectra collected using the R406 PMT (Fig. 1) from  $\sim 20 \mu\text{m}$  diameter regions of pressed pellets of finely ground olivine ( $\sim 10$  mol% Fe), orthopyroxene ( $\sim 10$  mol% Fe), and serpentine.

less sensitive than the R928 PMT detector, its spectral range includes the important  $\sim 1 \mu\text{m}$  "silicate" region (Fig. 1).

Preliminary data acquired with the R406 establish that olivine and pyroxene with as little as 10 mol% Fe can be readily detected (Fig. 12). Olivine and pyroxene are important minerals in chondritic IDPs. The relative abundances of these two minerals are used to classify anhydrous chondritic IDPs into "pyroxene" and "olivine" classes, and a third "layer silicate" class of chondritic IDPs is also recognized (Sandford and Walker, 1985). Since anhydrous "pyroxene" IDPs are usually dominated by low-Fe ( $< 1$  wt%) enstatite and forsterite (Bradley *et al.*, 1989; Bradley, 1994c), they are unlikely to exhibit a strong "silicate" absorption at  $\sim 1 \mu\text{m}$ . Similarly, "layer silicate" IDPs dominated by poorly crystallized smectite or serpentine are unlikely to exhibit strong silicate features. "Olivine" class IDPs, on the other hand, typically contain significant amounts of Fe-bearing olivine and pyroxene (Bradley *et al.*, 1989; Christofferson and Buseck, 1986; Zolensky and Barrett, 1994) and thus are expected to exhibit strong silicate features.

It has been suggested that the "olivine" class includes and is perhaps dominated by IDPs that were severely pulse heated during atmospheric entry (Sandford and Bradley, 1989; Bradley, 1994a). Similarly, IDPs (and polar micrometeorites) that were clearly strongly heated ( $> 1000^\circ\text{C}$ ) during atmospheric entry usually contain Fe-bearing olivines and pyroxenes. Thus, chondritic IDPs exhibiting strong  $\sim 1 \mu\text{m}$  silicate features are unlikely to belong to either the "pyroxene" or "layer silicate" classes. They are more likely "olivine" class IDPs and/or particles that were strongly heated during atmospheric entry, since both are likely to contain significant amounts of Fe-rich anhydrous silicates. This hypothesis will be tested in future studies.

The third goal of this study was to make a preliminary comparison between the reflectance properties of IDPs and asteroids. The ultimate goal is to determine the sources of IDPs by comparing their spectral properties with those of the various asteroid families. However to make such a comparison, it is necessary to assume that the properties of micrometer-sized particles are representative of the kilometer-sized objects from which they were derived. In the case of a fractionated parent body like the lunar regolith, the spectral properties of a  $10 \mu\text{m}$  feldspar crystal are hardly representative of the lunar regolith. On the other hand, the reflectance properties of bulk soils are largely determined by the finest material (i.e., the  $< 10 \mu\text{m}$  diameter size fraction; Pieters *et al.*, 1994). A  $10 \mu\text{m}$  particle

from a primitive, unfractionated body like an outer asteroid or comet may be representative of the parent body as a whole. For example, dust from comet Halley, the most primitive, unfractionated solar system body for which compositional data are available, was compositionally and mineralogically heterogeneous on a submicrometer scale (Jessberger *et al.*, 1988; Brownlee *et al.*, 1987; Lawler *et al.*, 1989; Bradley *et al.*, 1992).

Although Fig. 4 indicates that there is significant overlap between the spectral properties of CS and CP IDPs, data from all chondritic IDPs so far measured (~100) reveal that each class exhibits a distinctive trend (see Fig. 13). If "bright" CS IDPs (those dominated by single mineral grains) as well as those showing a near-IR fall-off (possibly from surficial magnetite) are ignored, "pristine" fine-grained CS IDPs are dark objects (<15% reflectivity) over the visible wavelength range 450–800 nm. Longwards of 500 nm, the spectra are generally flat with a tendency to fall off into the near-IR (Bradley, 1994a). W7030A15 is an example of a "pristine" CS IDP (Fig. 13, upper). Some CI and CM meteorites and main belt C-asteroids have spectral characteristics similar to CS IDPs between 450 and 800 nm (Gaffey *et al.*, 1993; Hiroi *et al.*, 1994a,b). From TEM studies, three CS IDPs have been mineralogically linked to CI and CM meteorite petrogenesis and a main-belt type C asteroid origin (Bradley and Brownlee, 1992; Keller *et al.*, 1992; Rietmeijer, 1992). However, there are many CS IDPs with "C-type" reflectance spectra that are mineralogically unlike CI and CM meteorites. Their diverse mineralogy supports the expectation that asteroidal IDPs

sample a broader range of (main belt) objects than CI and CM meteorites (Brownlee, 1994).

Most anhydrous CP IDPs are also dark objects (<10% reflectivity) in the VIS wavelength range 450–800 nm. Longwards of 500 nm, the spectra generally tend to rise steadily into the near-IR (Bradley, 1994a). W7035A5 is an example of a "pristine" CP IDP (Fig. 13, lower). Outer P and D asteroids are also dark (low albedo) objects whose spectra show a slight rise into the near-IR. Chondritic porous IDPs are the first identified meteoritic materials exhibiting VIS reflectivities similar to P and D asteroids. Bearing in mind that the reflectance spectra of outer asteroids are similar to those of comets (Jewitt and Luu, 1990), 16 out of 18 chondritic IDPs so far identified as cometary (using He release measurements) are classical CP IDPs (Brownlee *et al.*, 1995).

The most intriguing comparison between CP IDPs and outer asteroids concerns the C-rich particles. The flat low albedos of outer asteroids have been interpreted as evidence for a finely disseminated, absorbing material like C, and the redness of one particular object (Pholus) as evidence for a kerogen-like organic material (Binzel, 1992; Cruikshank and Brown, 1987; Luu *et al.*, 1994). The most C-rich CP IDPs are dark and spectrally red. Fragment 10 of Cluster IDP L2006 #14, which contains >90% C by volume is the most extreme example (Figs. 9 and 10). Whether fragment 10 contains organic material or not will be determined using two-step laser desorption mass spectroscopy (Clemett *et al.*, 1992, 1993). The albedo and shape of the spectrum from fragment 10 is similar to that of Pholus, the darkest and most spectrally red outer asteroid so far detected (Binzel, 1992; Luu *et al.*, 1994). Although carbonaceous material is clearly a cause of darkening and reddening in IDPs, other components like GEMS containing nanometer-size metal grains may also cause darkening (Bradley, 1994b). ("Metal blacks," nanometer grain-size metal powders, exhibit low albedos irrespective of their elemental compositions.) The distribution of C throughout an IDP may influence darkening; an IDP containing a continuous coating of C on its surfaces will be spectrally darker than one in which C is concentrated towards the center. Finally, fragment 37 of cluster IDP L2005 #8 (Fig. 8) shows that secondary magnetite also causes darkening.

## SUMMARY

The spectral reflectivities of chondritic IDPs have been measured using microscope spectrophotometry. This study shows that it is possible to make such measurements in the VIS wavelength range (450–800 nm), although interpretation of the indigenous properties of IDPs is complicated by particle effects (in the UV) and secondary magnetite on the surfaces of some IDPs. The following trends were observed. (1) Like carbonaceous chondrites, most fine-grained chondritic IDPs are spectrally dark with reflectivities from ~5 to 15% over the measurement range. (2) Chondritic IDPs containing large embedded or adhering single-mineral grains tend to be significantly brighter than IDPs with only fine-grained components. (3) Some hydrated (layer silicate-rich) chondritic smooth IDPs exhibit reflectance characteristics similar to CI and CM meteorites and main belt C asteroids. (4) Some anhydrous chondritic porous IDPs exhibit reflectance characteristics similar to outer P and D asteroids. The most C-rich CP IDPs are dark and some of them exhibit redness comparable with the outer asteroid object Pholus (Binzel, 1992). (5) It may be possible to identify strongly heated IDPs using reflectance spectroscopy by detecting surficial magnetite formed during atmospheric entry. (6) Spectra acquired from

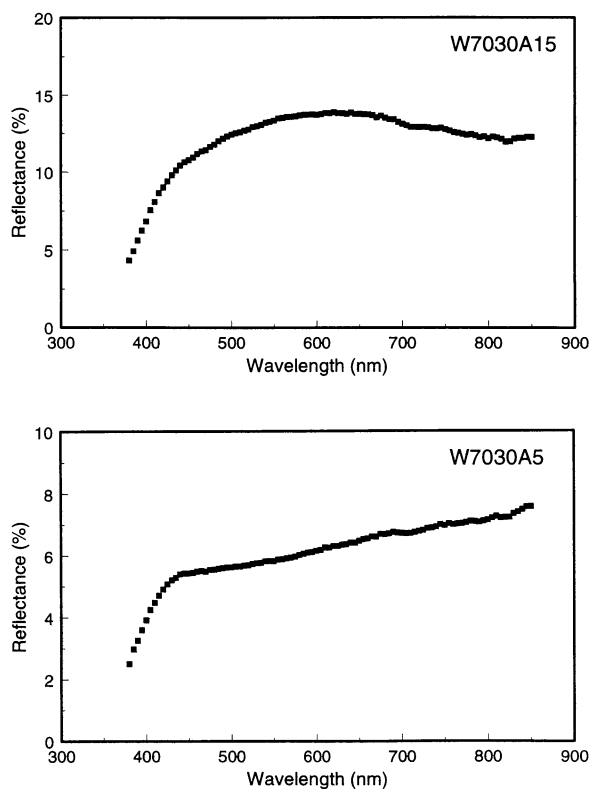


FIG. 13. Reflectance spectra of "pristine" chondritic IDPs (*i.e.*, fine-grained IDPs whose spectral properties are not influenced by large mineral grains or surficial magnetite formed during atmospheric entry). (Upper) Chondritic smooth (CP) IDP W7030A15. (Lower) Chondritic porous (CP) IDP W7030A5. (Data from Bradley, 1994a).



mineral standards indicate that the silicate mineralogy of IDPs can be probed using a PMT detector sensitive in the 1000 nm (1  $\mu\text{m}$ ) range.

Future studies will examine the influence of surface magnetite on IDPs in more detail. The silicate mineralogy of IDPs will be probed using the R5108 PMT to examine the  $\sim 1\ \mu\text{m}$  "silicate" region, and C-rich IDPs exhibiting low albedos and pronounced redness will be analyzed for organics.

**Acknowledgments**—This research was supported by NASA grants NASW-4831, NASW-3600, and NAS9-18992. We thank T. Callahan and R. S. Brown for technical assistance, M. Zolensky for helpful comments, and F. Vilas and C. Pieters for detailed reviews.

**Editorial handling:** S. Sandford

## REFERENCES

- ALLAMANDOLA L. J., SANDFORD S. A. AND WOPENKA B. (1987) Interstellar polycyclic aromatic hydrocarbons and carbon in interplanetary dust particles and meteorites. *Science* **237**, 56–59.
- BINZEL R. P. (1992) The optical spectrum of 5145 Pholus. *Icarus* **99**, 238–240.
- BINZEL R. P., SHUI X., SCHELTE J. B., STRUTSKIE M. F., MEYER M. R., KNEZEK P. AND BARKER E. S. (1993) Discovery of a main-belt asteroid resembling ordinary chondrite meteorites. *Science* **262**, 1541–1543.
- BRADLEY J. P. (1994a) Mechanisms of grain formation, post-accretionary alteration, and likely parent body environments of interplanetary dust particles (IDPs). In *Analysis of Interplanetary Dust* (eds. M. E. Zolensky, T. L. Wilson, F. J. M. Rietmeijer and G. J. Flynn) pp. 89–104. Amer. Inst. Phys. Conf. Proc. 310. AIP Press, Woodbury, New York.
- BRADLEY J. P. (1994b) Chemically anomalous, pre-accretionally irradiated grains in interplanetary dust from comets. *Science* **265**, 925–929.
- BRADLEY J. P. (1994c) Nanometer-scale mineralogy and petrography of fine-grained aggregates in anhydrous interplanetary dust particles. *Geochim. Cosmochim. Acta* **58**, 2123–2134.
- BRADLEY J. P. AND BROWNLEE D. E. (1992) An interplanetary dust particle linked directly to type CM meteorites and an asteroidal origin. *Science* **251**, 549–552.
- BRADLEY J. P., GERMANI M. S. AND BROWNLEE D. E. (1989) Automated thin-film analyses of anhydrous interplanetary dust particles in the analytical electron microscope. *Earth Planet. Sci. Lett.* **93**, 1–13.
- BRADLEY J. P., HUMECKI H. J. AND GERMANI M. S. (1992) Combined infrared and analytical electron microscope studies of interplanetary dust particles. *Ap. J.* **394**, 643–651.
- BRADLEY J. P., KELLER L. P., THOMAS K. L., VANDERWOOD T. B. AND BROWNLEE D. E. (1993) Carbon analyses of IDPs sectioned in sulfur and supported on beryllium films (abstract). *Lunar Planet. Sci.* **24**, 173–174.
- BRADLEY J. P., BROWNLEE D. E. AND KELLER L. P. (1994) Reflectance spectroscopy of individual interplanetary dust particles (abstract). *Lunar Planet. Sci.* **25**, 159–160.
- BRADLEY J. P., BROWNLEE D. E. AND KELLER L. P. (1995) Reflectance spectra (from 380–800 nanometers) of interplanetary dust particles (abstract). *Lunar Planet. Sci.* **26**, 161–162.
- BROWNLEE D. E. (1986) Cosmic dust: collection and research. *Ann. Rev. Earth Planet. Sci.* **13**, 147–173.
- BROWNLEE D. E. (1994) The origin of dust in the early solar system. In *Analysis of Interplanetary Dust* (eds. M. E. Zolensky, T. L. Wilson, F. J. M. Rietmeijer and G. J. Flynn), pp. 5–8. Amer. Inst. Phys. Conf. Proc. 310. AIP Press, Woodbury, New York.
- BROWNLEE D. E., OLSZEWSKI E. AND WHEELLOCK M. M. (1982) A working taxonomy for micrometeorites (abstract). *Lunar Planet. Sci.* **13**, 71–72.
- BROWNLEE D. E., WHEELLOCK M. M., TEMPLE S., BRADLEY J. P. AND KISSEL J. (1987) A quantitative comparison of comet Halley and carbonaceous chondrites at the submicrometer level (abstract). *Lunar Planet. Sci.* **18**, 133–134.
- BROWNLEE D. E., JOSWIAK D. J., LOVE S. G., BRADLEY J. P., NIER A. O. AND SCHLUTTER D. J. (1994) Identification and analysis of cometary IDPs (abstract). *Lunar Planet. Sci.* **25**, 185–186.
- BROWNLEE D. E., JOSWIAK D. J., SCHLUTTER D. J., PEPIN R. O., BRADLEY J. P. AND LOVE S. G. (1995) Identification of individual cometary IDPs by thermally stepped He release (abstract). *Lunar Planet. Sci.* **26**, 183–184.
- BURNS R. G. (1993) *Mineralogical Applications of Crystal Field Theory*. Cambridge University Press, New York, New York. 551 pp.
- CHRISTOFFERSON R. AND BUSECK P. R. (1986) Mineralogy of interplanetary dust particles from the "olivine" infrared class. *Earth Planet. Sci. Lett.* **78**, 53–66.
- CLEMETT S. J., MAECHLING C. R. AND ZARE R. N. (1992) Analysis of polycyclic aromatic hydrocarbons in seventeen ordinary and carbonaceous chondrites (abstract). *Lunar Planet. Sci.* **23**, 233–234.
- CLEMETT S. J., MAECHLING C. R., ZARE R. N., SWAN P. D. AND WALKER R. M. (1993) Identification of complex aromatic molecules in individual interplanetary dust particles. *Science* **262**, 721–725.
- CRUIKSHANK D. P. AND BROWN R. H. (1987) Organic matter on asteroid 130 Elektra. *Science* **238**, 183–184.
- DERMOTT S. F., JAYARMAN S., XU Y. L., GUSTAFSON B. A. S. AND LIOU J. C. (1994) A circumsolar ring of asteroidal dust in resonant lock with the Earth. *Nature* **369**, 719–723.
- FARINELLA P., GONCZI R., FROESCHLE C. AND FROESCHLE C. (1993) The injection of asteroid fragments into resonances. *Icarus* **101**, 174–187.
- FLYNN G. J. (1989) Atmospheric entry heating: A criterion to distinguish between asteroidal and cometary sources of interplanetary dust. *Icarus* **77**, 190–197.
- FLYNN G. J., SUTTON S. R., THOMAS K. L., KELLER L. P. AND KLOCK W. (1992) Zinc depletions and atmospheric entry heating in stratospheric cosmic dust particles (abstract). *Lunar Planet. Sci.* **23**, 375–376.
- GAFFEY M. J., BURBINE T. H. AND BINZEL R. P. (1993) Asteroid spectroscopy: Progress and perspectives. *Meteoritics* **28**, 161–187.
- GERMANI M. S., BRADLEY J. P. AND BROWNLEE D. E. (1990) Automated thin-film analyses of hydrated interplanetary dust particles in the analytical electron microscope. *Earth Planet. Sci. Lett.* **101**, 162–179.
- GRADIE J. AND TEDESCO E. (1982) Compositional structure of the asteroid belt. *Science* **216**, 1405–1407.
- GRADIE J. AND VERVERKA J. (1980) The composition of the Trojan asteroids. *Nature* **283**, 840–842.
- GRIMM R. E. AND MCSWEEEN H. Y., JR. (1993) Heliocentric zoning of the asteroid belt by aluminum-26 heating. *Science* **259**, 653–655.
- HIROI T., PIETERS C. M. AND ZOLENSKY M. E. (1993a) Comparison of reflectance spectra of C asteroids and unique C chondrites Y86720, Y82162, and B7904 (abstract). *Lunar Planet. Sci.* **24**, 659–660.
- HIROI T., PIETERS C. M., ZOLENSKY M. E. AND LIPSCHUTZ M. E. (1993b) Evidence of thermal metamorphism on the C, G, B and F asteroids. *Science* **261**, 1016–1018.
- JEWITT D. C. AND LUU J. X. (1990) CCD spectra of asteroids II. The Trojans as spectral analogs of cometary nuclei. *Astron. J.* **100**, 933–944.
- JESSBERGER E. K., CHRISTOFORIDIS A. AND KISSEL J. (1988) Aspects of the major element composition of Halley's dust. *Nature* **332**, 691–695.
- JOHNSON T. V. AND FANALE F. B. (1973) Optical properties of carbonaceous chondrites and their relationship to asteroids. *J. Geophys. Res.* **78**, 8507–8515.
- KELLER L. P., THOMAS K. L. AND MCKAY D. S. (1992) An interplanetary dust particle with links to CI chondrites. *Geochim. Cosmochim. Acta* **56**, 1409–1412.
- KELLER L. P., THOMAS K. L., BRADLEY J. P. AND MCKAY D. S. (1995) Nitrogen in interplanetary dust particles (abstract). *Meteoritics* **30**, 526–527.
- KELLER L. P., THOMAS K. L. AND MCKAY D. S. (1996) Mineralogical changes in IDPs resulting from atmospheric entry heating. *IAU Conf. Proc.*, in press.
- KURAT G., BRANDSTATTER F., PRESER T., KOEBERL C. AND MAURETTE M. (1993) Micrometeorites. *Russ. Geol. Geophys.* **34**, 132–147.
- LAWLER M. E., BROWNLEE D. E., TEMPLE S. AND WHEELLOCK M. M. (1989) Iron, magnesium, and silicon in dust from comet Halley. *Icarus* **80**, 225–242.
- LOVE S. G. AND BROWNLEE D. E. (1994) Peak atmospheric entry heating temperatures of micrometeorites. *Meteoritics* **29**, 69–70.
- LUU J., JEWITT D. C. AND CLOUTIS E. (1994) Near infrared spectroscopy of primitive solar system objects. *Icarus* **109**, 133–144.
- MAURETTE M., KURAT G., PERREAU M. AND ENGRAND C. (1993) Microanalyses of Cap-Prudhomme Antarctica micrometeorites. *Microbeam Analysis* **2**, 239–251.
- NIER A. O. (1994) Helium and Neon in interplanetary dust particles. In *Analysis of Interplanetary Dust* (eds. M. E. Zolensky, T. L. Wilson, F. J. M. Rietmeijer and G. J. Flynn), pp. 115–126. Amer. Inst. Phys. Conf. Proc. 310. AIP Press, Woodbury, New York.
- NIER A. O. AND SCHLUTTER D. J. (1990) Helium and Neon isotopes in stratospheric particles. *Meteoritics* **25**, 263–267.
- PIETERS C. M. AND MCFADDEN L. A. (1994) Meteorite and asteroid reflectance spectroscopy. *Annu. Rev. Earth Planet. Sci.* **22**, 457–497.



- PIETERS C. M., FISCHER E. M., RODE O. D. AND BASU A. (1993) Optical effects of space weathering on lunar soils and the role of the finest fraction (abstract). *Lunar Planet. Sci.* **24**, 1143.
- REACH W. T., FRANZ B. A., WEILAND J. L., HAUSER M. G., KELSALL T. N., WRIGHT E. L., RAWLEY G., STEMWEDEL S. W. AND SPEISMAN W. J. (1995) Observational confirmation of a circumsolar dust ring by the COBE satellite. *Nature* **374**, 521–523.
- RIETMEIJER F. J. M. (1992) Interplanetary dust particle L2005T12 linked directly to type CM chondrite petrogenesis (abstract). *Lunar Planet. Sci.* **23**, 1153–1154.
- SANDFORD S. A. AND BRADLEY J. P. (1989) Interplanetary dust particles collected in the stratosphere: Observations of atmospheric heating and constraints on their inter-relationships and sources. *Icarus* **82**, 146–166.
- SANDFORD S. A. AND WALKER R. M. (1985) Laboratory infrared transmission spectra of individual interplanetary dust particles from 2.5 to 25 microns. *Ap. J.* **291**, 838–851.
- SCHRAMM L. S., BROWNLEE D. E. AND WHEELLOCK M. M. (1989) Major element composition of stratospheric micrometeorites. *Meteoritics* **24**, 99–112.
- THOLEN D. J. (1984) Asteroid taxonomy from cluster analysis of photometry. Ph.D. Thesis, University of Arizona. 150 pp.
- THOMAS K. L., KELLER L. P., BLANFORD G. E. AND MCKAY D. S. (1994) Quantitative analyses of carbon in anhydrous and hydrated interplanetary dust particles. In *Analysis of Interplanetary Dust* (eds. M. E. Zolensky, T. L. Wilson, F. J. M. Rietmeijer and G. J. Flynn), pp. 165–172. Amer. Inst. Phys. Conf. Proc. 310. AIP Press, Woodbury, New York.
- THOMAS K. L., BLANFORD G. E., CLEMETT S. J., FLYNN G. J., KELLER L. P., MCKAY D. S., MESSENGER S., NIER A. O., SCHLUTTER D. J., SUTTON S. R., WARREN J. L. AND ZARE R. N. (1995a) An asteroidal breccia: The anatomy of a cluster IDP. *Geochim. Cosmochim. Acta* **59**, 2797–2815.
- THOMAS K. L., KELLER L. P., CLEMETT S. J., MCKAY D. S., MESSENGER S. AND ZARE R. N. (1995b) Hydrated cluster particles: Chemical and mineralogical analyses of fragments from two interplanetary dust particles (abstract). *Lunar Planet. Sci.* **26**, 1407–1408.
- VILAS F. AND GAFFEY M. J. (1989) Phyllosilicate absorption features in main-belt and outer asteroid reflectance spectra. *Science* **246**, 790–792.
- VILAS F. AND SMITH B. A. (1985) Reflectance spectrophotometry (0.5–1.0  $\mu\text{m}$ ) of outer belt asteroids: Implications for primitive, organic solar system material. *Icarus* **64**, 503–516.
- ZOLENSKY M. AND BARRETT R. (1994) Olivine and pyroxene compositions of chondritic interplanetary dust particles. In *Analysis of Interplanetary Dust* (eds. M. E. Zolensky, T. L. Wilson, F. J. M. Rietmeijer and G. J. Flynn), pp. 105–114. Amer. Inst. Phys. Conf. Proc. 310. AIP Press, Woodbury, New York.